DOI 10.4430/bgo00421

Recent earthquakes (2000-2021) in and around the Friuli Venezia Giulia region (NE Italy) and quality improvements of the OGS network monitoring capabilities

D. Sandron[1], A. Rebez[1], A. Tamaro[1] and D. Slejko[2]

[1] *National Institute of Oceanography and Applied Geophysics - OGS, Trieste, Italy*
[2] *Affiliate of National Institute of Oceanography and Applied Geophysics - OGS, Trieste, Italy*

(Received: 24 January 2023; accepted: 11 May 2023; published online: 25 August 2023)

ABSTRACT Regular monitoring of the seismicity in north-eastern Italy began in 1977, one year after the strong earthquake that caused about 1000 victims in Friuli. Over the years, the monitoring network operated by OGS has increased, today reaching a consolidated level in terms of geometry and number of stations. Furthermore, the entire data acquisition and processing system, which has changed over the years, is currently also highly robust. After the huge number of studies on the 1976 seismic sequence and on the regional seismicity developed in the 1970s and 1980s, the present paper illustrates a comprehensive work on the subject since the beginning of the 21st century. With this work, we take up the thread and analyse the evolution of seismicity in the first two decades of the 21st century (2000-2021). As part of the study, we took a retrospective look at the qualitative development of the data provided by OGS over time, basically focusing on the earthquake catalogue obtained by the network recordings and developing a new relation for calculating the duration magnitude.

Key words: regional seismicity, north-eastern Italy, catalogue completeness, location accuracy, magnitude homogenisation.

1. Introduction

It is common knowledge (e.g. Slejko *et al*., 1999) that north-eastern Italy corresponds to the northernmost part of the Adriatic microplate, which collides and rotates anti-clockwise with respect to the Eurasian plate. The N-S convergent movement induces a considerable state of stress and consequently, the pre-Alpine belt is one of the most seismically active districts in Italy (e.g. Slejko *et al*., 1989; Carulli *et al*., 1990; Del Ben *et al*., 1991). Specifically, the eastern Alps are the most seismic segment of the Alps, and their activity has been fairly well documented since the Middle Ages due to the presence of towns established during the Roman period and developed in the following centuries (e.g. Belluno, Cividale, Ljubljana, and Trieste). The instrumental data collection was, and still is, particularly abundant due to the presence of some seismographic stations [e.g. Trieste, Ljubljana, Pula (Pola), Rijeka (Fiume), Padova, Venezia, and Treviso], which have been operating since the early 20th century.

Countless studies have been conducted over the years on the seismicity in north-eastern Italy, following the destructive earthquake of 1976. This date marked a watershed not only for the development of local seismology, but motivated on the one hand the foundation of the

© 2023 - OGS

National Civil Protection (Rebez *et al*., 2018) and on the other, the beginning of regional seismic monitoring entrusted to the Osservatorio Geofisico Sperimentale (OGS, today Istituto Nazionale di Oceanografia e Geofisica Sperimentale - OGS). Thanks also to these studies on regional seismicity (e.g. Slejko *et al*., 1989; Carulli *et al*., 1990; Del Ben *et al*., 1991), the seismic activity in this region is rather well documented and the seismic areas are identified. Major seismicity occurs along the piedmont belt, from Cividale to Belluno, reaching its maximum in central Friuli; other seismic areas are in western Slovenia and, to a minor extent, in southern Austria (Fig. 1). The main events (Table 1) affected the present border between Italy and Austria in 1348 (Caracciolo *et al*., 2021) and 1690 (Cergol and Slejko, 1991), the border with Slovenia in 1511 (Camassi *et al*., 2011), the Veneto piedmont area in 1695, 1873 (Peruzza *et al*., 1989), and 1936 (Andreotti, 1937; Giacchetti *et al*., 1987), and central Friuli in 1928 (Gortani, 1928; Cavasino, 1929) and 1976 (Slejko, 2018). More information on all the main events in the study region can be found in Guidoboni *et al*. (2018, 2019).

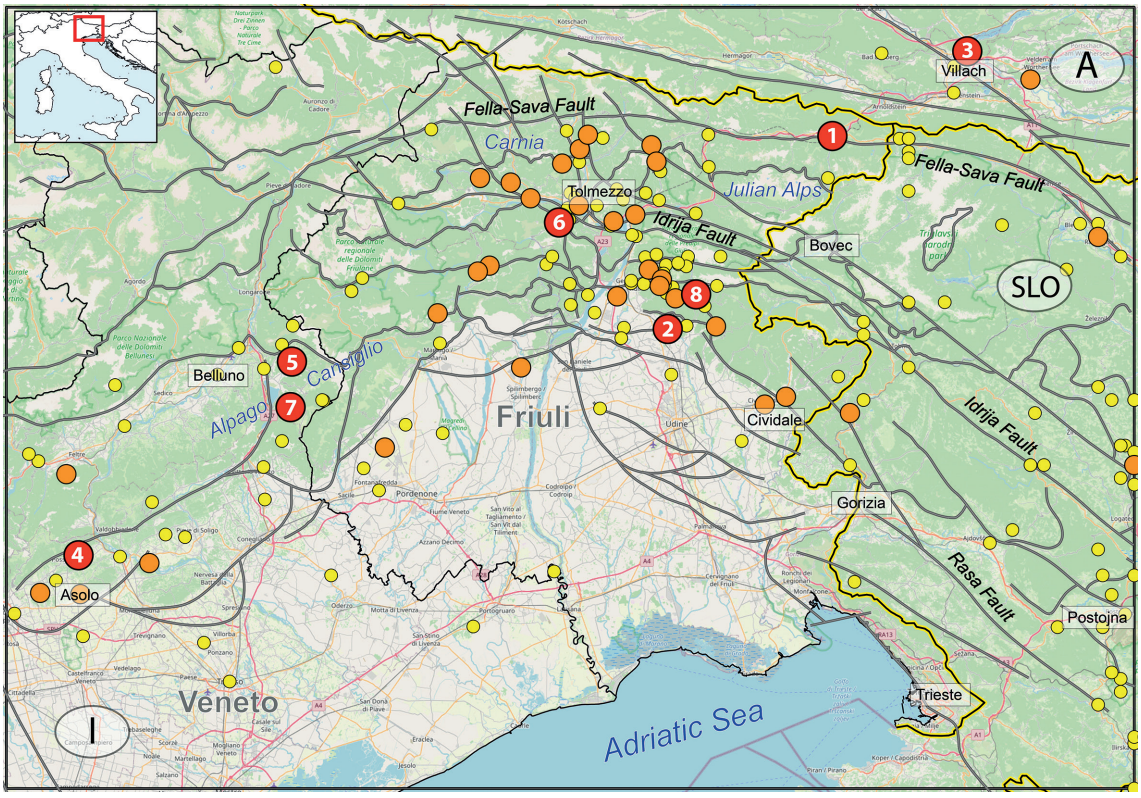

Fig. 1 - Earthquakes with an M_w larger than, or equal to, 4.0 occurring in the eastern Southern Alps from the year 1000 to 5 May 1977. The data are extracted from the CPTI catalogue (Rovida *et al*., 2020, 2022) except for event n. 8, whose epicentral parameters are taken from Slejko (2018). Red numbered dots show earthquakes with an M_w larger than, or equal to, 6.0 (Table 1), orange dots with an M_w larger than, or equal to, 5.0, and yellow dots with an M_w larger than, or equal to, 4.0. Main faults are taken from Poli and Zanferrari (2018).

On 6 May 1977, the first five stations of a regional network (today the North-East Italy Seismic Network, OX network code at the International Federation of Digital Seismograph Networks, FDSN, http://www.fdsn.org) were installed by the OGS, initially to follow the evolution of the 6 May 1976

Table 1 - Earthquakes with an M_W larger than, or equal to, 6.0 occurring in north-eastern Italy and western Slovenia from the year 1000 to 5 May 1977. The data are extracted from the CPTI catalogue (Rovida *et al.*, 2020, 2022) except for event n. 8, whose epicentral parameters are taken from Slejko (2018).

No.	Year	Mo	Da	Ho	Mi	Epicentral Area	Lat. N (°)	Lon. E (°)	I_0 (MCS)	*Mw*
1	1348	01	25			Julian Alps	46.504	13.581	9	6.6
2	1511	03	26	15	30	Friuli-Slovenia	46.209	13.216	9	6.3
3	1690	12	04	14		Villach, Carinthia	46.633	13.880	8-9	6.2
4	1695	02	25	05	30	Asolano	45.861	11.910	10	6.4
5	1873	06	29	03	58	Alpago-Cansiglio	46.159	12.383	9-10	6.3
6	1928	03	27	08	32	Carnia	46.372	12.975	9	6.0
7	1936	10	18	03	10	Alpago-Cansiglio	46.089	12.380	9	6.1
8	1976	05	06	20	00	Friuli	46.262	13.279	9-10	6.5

earthquake and, later, to monitor the seismicity of the region (e.g. Priolo *et al.*, 2005; Peruzza *et al.*, 2015; Bragato *et al.*, 2021). In such a way, a huge number of earthquakes has been recorded and the parameters of the located events have allowed a deep investigation of the regional seismicity.

A new representation of seismicity is proposed here (Fig. 2) to highlight the areas with the largest release of seismic energy. The study region has been subdivided into hexagonal cells of

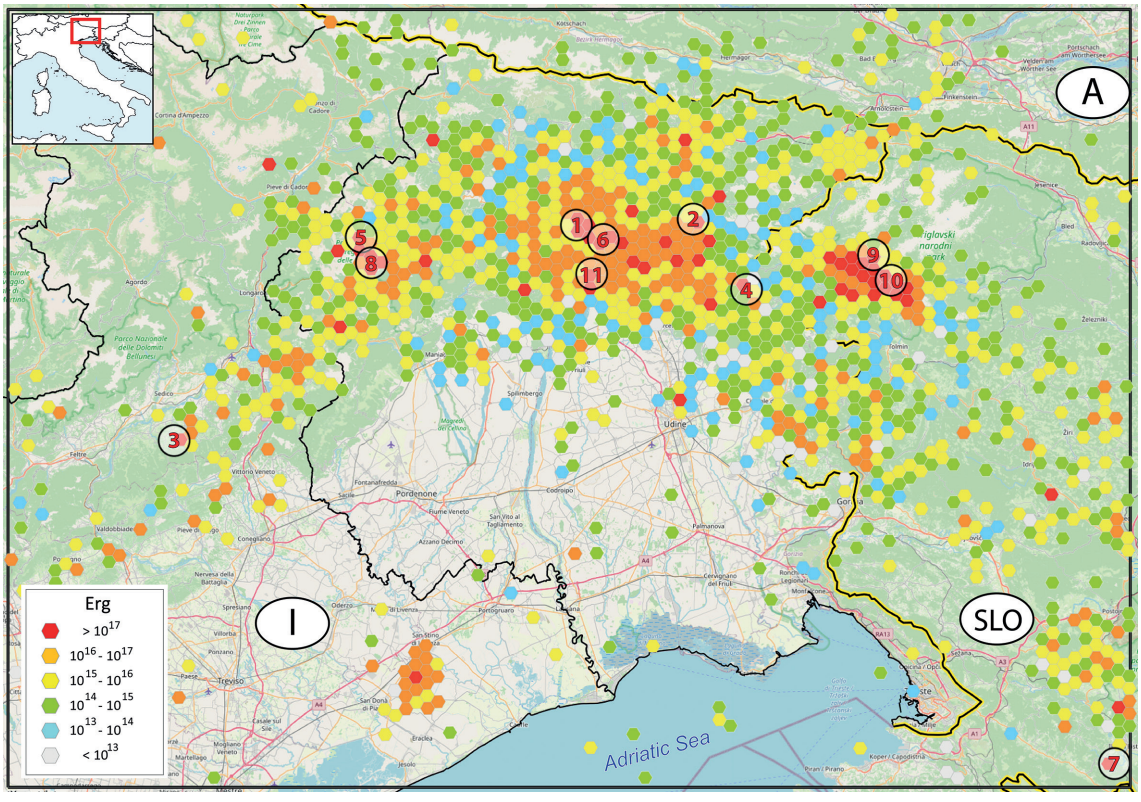

Fig. 2 - Cumulative seismic energy released in the period 6 May 1977 – 31 December 1999 from the OX network catalogue. Earthquakes with an M_D larger than, or equal to, 4.0, listed in Table 2, are highlighted with numbered circles.

1.25-km length side. A hexagonal grid provides better readability than a standard rectangular grid, improving the visual clarity of spatial distributions and the homogeneity of cells in a neighbourhood, the pattern being fully symmetrical in terms of distance (Iurcev *et al*., 2021). Within each cell the cumulative energy has been calculated (Reiter, 1990) from the duration magnitude (M_D) reported in the OX network catalogue (see later for a complete description of this catalogue). The features of the seismicity located by OGS in the period 1977-1999 (Fig. 2) repeat those of the historical seismicity. In fact, the bulk of events follows the piedmont belt from Veneto (Alpago - Cansiglio) to Slovenia (Bovec and Postojna areas) with larger quakes in central Friuli (Table 2). It is worth mentioning that part of the seismicity still corresponds to the tail-end of events following the M_W 6.5 Friuli earthquake that, with the subsequent seismic sequence, is documented in several specific studies (e.g. Finetti *et al*., 1979; Poli *et al*., 2002; Carulli and Slejko, 2005; Rebez *et al*., 2018; Slejko, 2018). Likewise, the energy cluster just across the Slovenian border is related to the seismicity following the strong event that struck Bovec in 1998 (Bajc *et al*., 2001).

Table 2 - Earthquakes with an M_D larger than, or equal to, 4.0 occurring in north-eastern Italy and western Slovenia from 6 May 1977 to 31 December 1999. The data are extracted from the OX network catalogue.

No.	Date	Or. Time	Lat. N (°)	Lon. E (°)	M_D	Place
1	1977-09-16	23:48:06	46.370	13.016	5.2	Tolmezzo, Friuli
2	1979-04-18	15:19:18	46.379	13.276	4.8	Chiusaforte, Friuli
3	1980-10-14	13:33:27	46.038	12.120	4.0	Mel, Veneto
4	1983-02-10	22:30:34	46.271	13.395	4.2	Uccea, Friuli
5	1986-08-29	14:57:01	46.352	12.537	4.0	Mt. Pramaggiore, Friuli
6	1988-02-01	14:21:38	46.348	13.076	4.1	Tolmezzo, Friuli
7	1995-05-22	12:50:31	45.537	14.215	4.0	Ilirska Bistrica, Slovenia
8	1996-04-13	13:00:22	46.312	12.559	4.3	Claut, Friuli
9	1998-04-12	10:55:32	46.324	13.678	5.6	Bovec, Slovenia
10	1998-05-06	02:53:00	46.285	13.717	4.6	Kuk, Slovenia
11	1998-05-28	09:32:19	46.295	13.050	4.1	Trasaghis, Friuli

All available geological, geophysical, and seismological data led to formulating a seismotectonic model for north-eastern Italy (Slejko *et al*., 1989), in which the seismicity is concentrated in northern Friuli, where the current uplift relates to the crustal thickening or doubling and the Fella-Sava subvertical fault acts as a mechanical disengagement that renders the northernmost part of the Southern Alps inactive.

Carulli *et al*. (1990) expanded eastwards the Slejko *et al*. (1989) seismotectonic model, observing that the seismicity occurs within a narrow area between the present front of the External Dinarides and the subvertical Idrija fault, where a large crustal thickening has been observed.

Further analysis of the regional seismicity at the Alps – Dinarides contact was performed by Del Ben *et al*. (1991), who identified active seismotectonic elements in some transpressive strike-slip and thrust faults, among which the major ones are the Idrija and Rasa faults.

A good quality data set of 479 hypocentral locations and 123 fault plane solutions, based on the recordings of the OX seismometric network between 1977 and 1999, was obtained and used (Poli *et al*., 2002) to check the more recent seismogenic interpretation associated with the

area. The 1977-1999 seismicity appears distributed in a large crustal volume, with an evident westward shift of the maximum seismic activity, possibly caused by the 1976 sequence.

Galadini *et al*. (2005) defined the active faulting framework of the eastern Southern Alps and identified the main seismogenic faults responsible for the major earthquakes using new geomorphological and structural data. All the active faults they detected in the investigated area are thrust segments of the complex thrust system, which has led to the latest building of the eastern Southalpine chain.

We redirect the reader to a couple of papers focusing on the subdivision of the Friuli Venezia Giulia and Veneto regions, part of western Slovenia too, into seismic districts, according to seismological data and seismotectonic features (Sugan and Peruzza, 2011; Bressan *et al*., 2019). In those papers, a summary of the body of knowledge on the relation between the space-time aspects of seismicity and the geological-structural framework can be found. Seismogenic zonations suitable for seismic hazard assessment can be found in Slejko *et al*. (2011).

To some extent, the present paper is the final stage of a long process of revisiting the entire seismic monitoring activity conducted by OGS throughout its history. A path that first saw the recovery and analysis of historical seismicity from the beginnings of instrumental seismology (early 20th century) recorded by the Trieste seismological station (the only one in operation in this easternmost end of Italy) before the strong Friuli earthquake of 6 May 1976 (Sandron *et al*., 2014). Subsequently, based on the data of the Trieste station, equipped since 1972 with an original Wood-Anderson torsional seismograph (Sandron *et al*., 2015), the formula of Rebez and Renner (1991) for calculating M_D, still used today in routine and standard form, also to maintain continuity with the past, was recalibrated (Sandron *et al*., 2018), albeit with significant limitations. Because since 2015 OGS has also been providing local magnitude (M_L) values (based on waveform amplitude) for the regional events, a useful and large integration of data is here used to upgrade the relation between earthquake magnitude and waveform duration.

2. The OX network catalogue

Since 1977, OGS has been producing the seismological bulletin of its network. Today, OGS manages the north-eastern Italy monitoring system (SMINO), fulfilling the institutional tasks of surveillance and research on seismic activity in north-eastern Italy, also for civil protection purposes (Bragato *et al*., 2021). SMINO, an infrastructure of national importance, consists of the OX seismic network, a strong motion network, and a geodetic monitoring network. With national and international networks in neighbouring countries, real-time data are exchanged and information on seismic events is disseminated to the public through a dedicated web portal [Real Time Seismology (RTS): https://rts.crs.ogs.it]. Seismic bulletins and the related catalogue are published regularly (yearly files) in electronic format only and are accessible at the web portal of the seismological research centre (www.crs.ogs.it/bollettino_new/).

Over the years, the area of interest and the method of analysis have been evolving following the expansion of the network as well as its technical development (e.g. the passage from analog to digital recordings). The bulletin has also undergone one major revision (Renner, 1995) and several minor revisions aimed at correcting the errors and maintaining, as much as possible, the homogeneity of the data over the years (e.g. applying the same M_D formulae to all earthquakes). This bulk of data, downloaded from the RTS portal, is here referred to as the OX network catalogue and is used in the following elaborations.

Inside the geographical coordinates 45.5° to 46.7° N and 11.75° to 14.25° E, considered here as

the study region, and for the analysed period (6 May 1977 to 31 December 2021), the OX network catalogue consists of 23,873 records in the M_D range 0.0-5.6. Most of the seismic activity concentrated over time in this study region, namely the geographical area for which OGS is responsible for seismic monitoring since the installation and progressive development of its seismic network.

In Fig. 3, the number of seismic events is sampled per year (blue histogram): 1589 earthquakes were recorded in 1979, and more than 200 of this inexplicably large number of events are linked to a seismic sequence triggered by the M_D 4.8, 18 April earthquake (Table 2); then, there is a progressive and constant decrease of annual recorded earthquakes until the late 1980s. The average annual number of earthquakes in the decade 1987-1997 is almost constant at around 200. The peaks in 1998 and 2004 are related to the two strong events which struck Bovec in Slovenia (Fig. 2). Applying a declustering algorithm [according to the space-time windows specially defined for the study region (Slejko and Rebez, 2002)] reduces the catalogue to 13,112 events and these peaks disappear (red histogram in Fig. 3). After 2004, there is a gradual increase in the number of recorded earthquakes up to about 1000 per year from 2018 to 2021. However, these events can be considered as background seismicity, not linked to the clustering of stronger events (even the red line has an increasing trend).

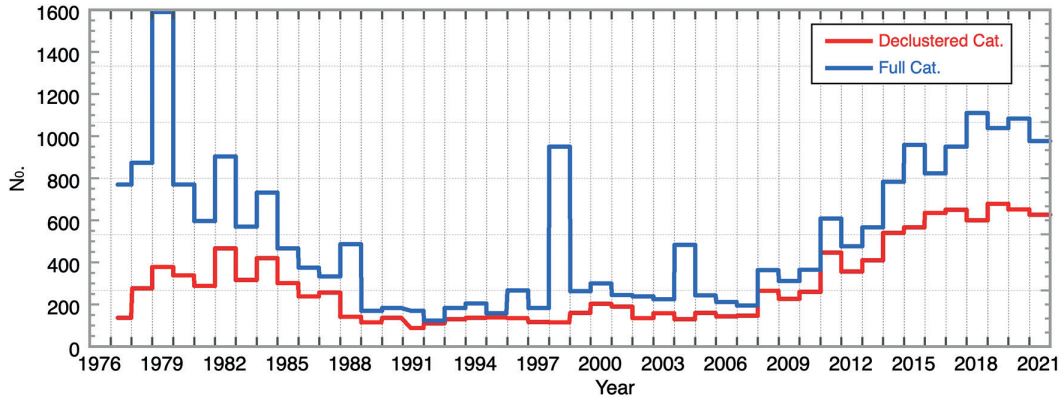

Fig. 3 - Number of earthquakes per year (1977-2021) inside the study area (45.5° - 46.7° N and 11.75° - 14.25° E) in the OX network complete (blue line) and declustered (red line) catalogues.

2.1. Accuracy of earthquake locations

The original code HYPO71 (Lee and Lahr, 1975) is traditionally used for earthquake location. Some of the program parameters have been modified to adapt the location procedure to the seismicity characteristics of the area of application (Sandron *et al.*, 2014). These parameters provide information on the reliability of the earthquake locations, and they are: RMS (the root-mean-square travel time residual, in seconds), ERH and ERZ (the horizontal and vertical standard errors in km), GAP (the largest azimuthal gap between azimuthally adjacent stations in degrees), and No (the number of station readings). According to some well-known 'rules of thumb' [summarised in Husen and Hardebeck (2010) and references therein] based upon a number of these parameters, a well-constrained hypocentre location should have: GAP < 180°; at least eight travel time arrivals (of which at least one is an S-wave arrival), and at least one of which within a focal depth distance from the epicentre; a correctly timed S-wave arrival recorded within 1.4 focal depth distance provides a unique constraint on focal depth.

A synoptic overview over time of some of these parameters is shown in Fig. 4, via an outlier box plot. The box is drawn from the 25th percentile to the 75th percentile with a horizontal line, in the middle, to denote the median (50th percentile). The whiskers are based on the 3rd quartile minus the 1st quartile value; outside this boundary, data points are plotted as outliers (see more details in the caption of Fig. 4).

The median value of RMS is equal to 0.14 s; 75% of the entire data set has a value less than, or equal to, 0.22 s (Fig. 4a). In the early years of network operation (1977–1982), the value was very low (around 0.1 s) and with very narrow boxes. Between the end of the 1980s and the beginning of the 2000s, as well as noticing a certain fluctuation of the value however on higher values, the data boxes are generally wider. Of note are an absolute RMS minimum for 2004 (0.06 s) and a substantial stabilisation (about 0.15 s) of the parameter's value from 2010 onwards.

The average standard error on the horizontal location (ERH) has undergone very small oscillations in time (Fig. 4b): from the beginning of the recordings the average value settled around 1 km for 10 years. During the 1990s, there are slight fluctuations with an increase up

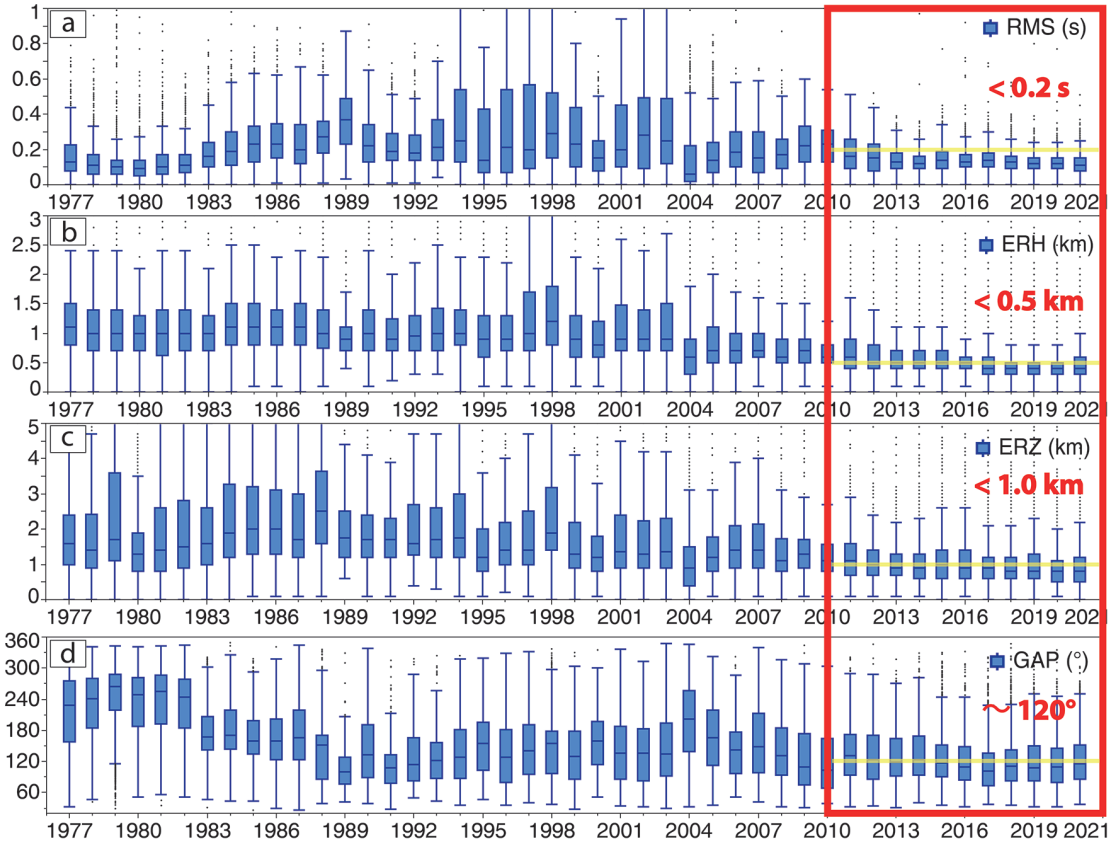

Fig. 4 - A synoptic overview over time (1977 – 2021) via box plot of the HYPO71 (Lee and Lahr, 1975) earthquake location parameters: a) RMS (the root-mean-square travel time residual, in seconds), b) ERH and c) ERZ (the horizontal and vertical standard errors in km); d) GAP (the largest azimuthal gap between azimuthally adjacent stations in degrees). The box is drawn from the 25th percentile to the 75th percentile with a horizontal line, drawn in the middle, to denote the median (50th percentile). The whisker's length is 1.5´IQR (Tukey fence), where IQR is the interquartile range, stopping at the minimum and/or maximum value when this extreme is outside the Tukey fence. Outliers are the values outside the Tukey fence. The red box highlights the period of the best performance of the OX network and the related mean values (see Fig. 5).

to 1.2 km in 1998 and down to 0.6 km in 2004. Then, the trend stabilises after 2010 with a progressive decrease towards a consolidated value around 0.5 km (0.4 km for 2017 to 2020). The median ERH value is equal to 0.7 km; 75% of the data have an ERH less than, or equal to, 1.1 km.

The average error on the focal depth (ERZ) shows fluctuating values between 1.5-2.5 km until 2004 when there is a sharp decrease (<1 km) and a progressive stabilisation around a value of 1 km. The median ERZ is equal to 1.2 km, and 75% of the entire data set has a value less than, or equal to, 2 km (Fig. 4c).

Also, for other parameters such as the average focal depth, the minimum station distances or the number of phases read, a substantial stable trend is shown starting from 2010. This is the date of maximum coverage of the network, after which its geometry remained substantially unchanged, along with the procedure of data acquisition and processing achieving a sort of standardisation. This is particularly evident analysing the GAP parameter (Fig. 4d). Until 1982, the network consisted of a core of 7 stations (Fig. 5; see later about the time-space evolution of the network) installed in the epicentral zone of the Friuli earthquake (Renner, 1995; Sandron *et al*., 2018) and the average GAP value was in the 240-260° range. In 1983, three stations were added and, then, another seven in 1988, as a result producing a sharp drop in the GAP to 160-170°. In the years that followed, the geometry of the network underwent further changes, and its configuration remained consolidated after 2010, with a median value of less than 120°. Overall, the average GAP value is equal to 148° with 75% of the locations within 217° and after 1983 this average value reduces to 160° (Fig. 4d).

The focal depth is generally the least constrained parameter of the HYPO71 location program (Husen and Hardebeck, 2010). Since the determination of focal depth of local earthquakes is made using direct arrivals**,** to calculate accurate values, the earthquake must occur within the network geometry and the epicentral distance to the closest station must be shorter than about 1.5 times the quake focal depth. In our case, the median interstation distance is equal to 25 km, so the location accuracy is very good for earthquakes with focal depth not exceeding 15 km. In the data set here analysed, the median value of the hypocentral depth is equal to 8.5 km.

2.2. The magnitude of completeness

The magnitude of completeness (*Mc*) is defined as the lowest magnitude threshold at which 100% of earthquakes in a space-time volume are detected (Mignan and Woessner, 2012, and reference therein). *Mc* is often estimated by fitting a Gutenberg-Richter (G-R) model to the observed frequency-magnitude rates and the lowest magnitude for which the rates deviate from the G-R law is taken as *Mc*.

Changes in the *Mc* value over time are closely related to the evolution of the seismic network geometry, because of the installation of new stations or, equally, the closure or relocation of pre-existing ones. The greatest fluctuations in *Mc* are, generally, due to aftershock sequences after large earthquakes. In our case, this eventuality is not contemplated as our analysis is conducted on the declustered OX network catalogue. Other types of changes involving the OX network regard the upgrading of hardware or software.

The maximum curvature technique [MAXC: Wiemer (2001)] is a quick and simple method to estimate *Mc* and consists of defining the point of maximum curvature by calculating the maximum value of the first derivative of the frequency-magnitude distribution (FMD).

The dark grey line in Fig. 5 represents our result obtained via the software package Zmap [version 7.1: http://www.seismo.ethz.ch/en/research-and-teaching/products-software/software/ZMAP/, Reyes and Wiemer (2019)]: the minimum number of events considered,

equal to approximately an average number of earthquakes per year, is 200. An overlap of 5%, a magnitude binning of 0.1, and a bootstrap of 200 was applied to the entire data set. In practice, *Mc* corresponds to the magnitude bin with the highest frequency of events in the non-cumulative FMD, as is quite evident in the density plot of Fig. 5.

The transition phases in the network are well-identified and show clear shifts in the estimates of *Mc*. More precisely, Fig. 5 shows an *Mc* value around 1.0 for the whole study region in the last decade while a value larger than 1.5 remains associated with the period 1985-2010. The low value (less than 1.0) during the very first years of the regional monitoring (1977-1982) must be intended related only to the epicentral area of the 1976 sequence, where the first stations were deployed. Gentili *et al*. (2011) found an *Mc* value of 1.5 for central Friuli for the whole period of their investigation (1977-2007).

We recall in the following some significant changes suffered by the OX network.

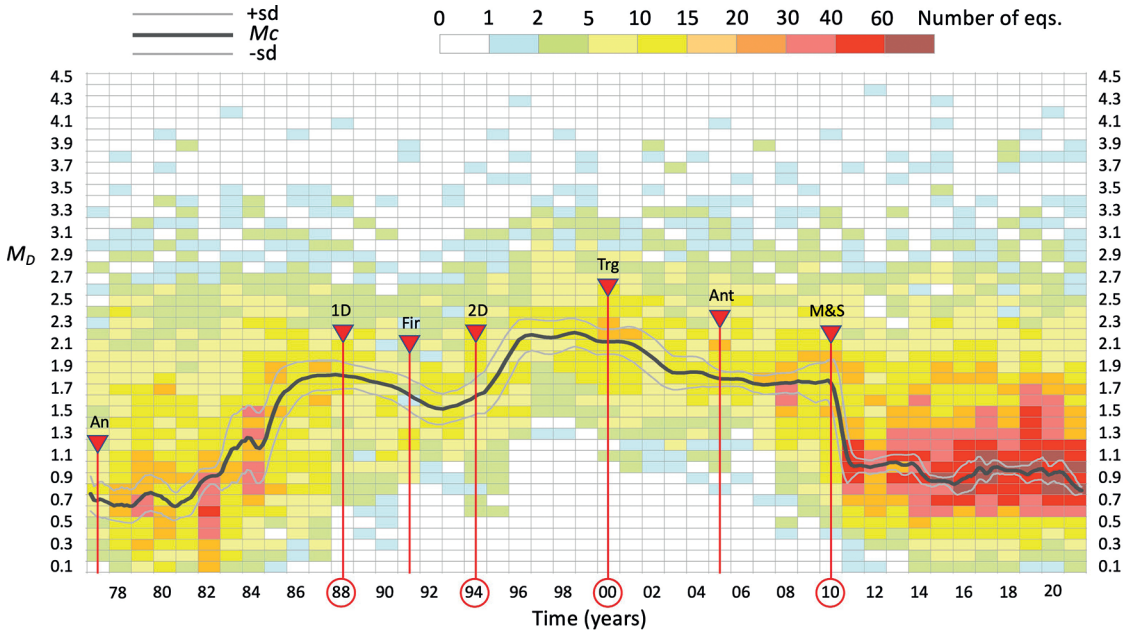

Fig. 5 - *Mc* synoptic overview over time (1977–2021), *Mc* (obtained by the maximum curvature technique) is the dark grey line drawn over a counter plot of earthquakes per year binned in 0.1 magnitude classes. The vertical lines identify the main dates when the OX network was modified. An = start of the analog network; 1D = first digital acquisition system; Fir = fire accident; 2D = second generation of digital acquisition system; Trg = improved trigger system; Ant = gradual introduction of the Antelope software; M&S = improvement of Antelope location parameters.

2.2.1. Temporal evolution of the network extension

The first core of stations in the Friuli Venezia Giulia region was installed on 6 May 1977 in the epicentral area (i.e. north of Udine and in the pre-Alpine arc) of the M_W 6.5 earthquake, which occurred exactly one year earlier. Until 1982, the network (red squares in Fig. 6) consisted only of this initial nucleus of stations (BAD, BOO, BUA, COLI, MPRI, RCL, UDI) plus the World Wide Standardized Seismographic Network (WWSSN) station of Trieste (TRI), active since 1963 (blue circle in Fig. 6). In 1981, five new stations from the neighbouring province of Trento plus a first station in the Veneto region (all outside Fig. 6) joined the network, with comprehensive

management by OGS. Extensions of the network took place in 1983, with the addition of three stations (CAE, DRE, ZOU), and in 1985, with the deployment of the station TLI, located in a 100-m deep well (orange squares in Fig. 6). A further nine stations were added in 1988 (green diamonds in Fig. 6): six of which in Friuli (CSM, CSO, CSZ, LSR, MLN, PLRO) and three in Veneto (AFL, FAU, MTLO). The stations CSM and MLN were added in 1994-1995 and, in the meanwhile, RCL was decommissioned. The station UDI had already been closed in 1990. A new impulse occurred in the first decade of the 2000s with the deployment of six stations in Friuli and eight in Veneto (azure triangles in Fig. 6, four stations in Veneto are outside the map). The OX network has not been modified since 2012, with the exception of the installation of two new stations (blue triangles in Fig. 6) in Veneto (APGO, MGBU). More details can be found at the RTS web portal (https://rts.crs.inogs.it/it/project/1_mappa.html), in Priolo *et al*. (2005), and Bragato *et al*. (2021).

2.2.2. Temporal evolution of the network technology

The first activation of permanent telemetry dates back to 1982-1983. At that time, four stations were still recording on thermosensitive paper (see small pentagons in Fig. 6) and were all dismissed in 1987. The first core of the network consisted of 1-s geophones (Mark LC4-1D). Between 1982-1983, the sensors were replaced by Willmore MKIIIA seismometers (An in Fig. 5). In 1987, the analog recording system was gradually replaced by a digital acquisition system with a trigger set to three stations (1D in Fig. 5). A fire accident caused a 6-month network

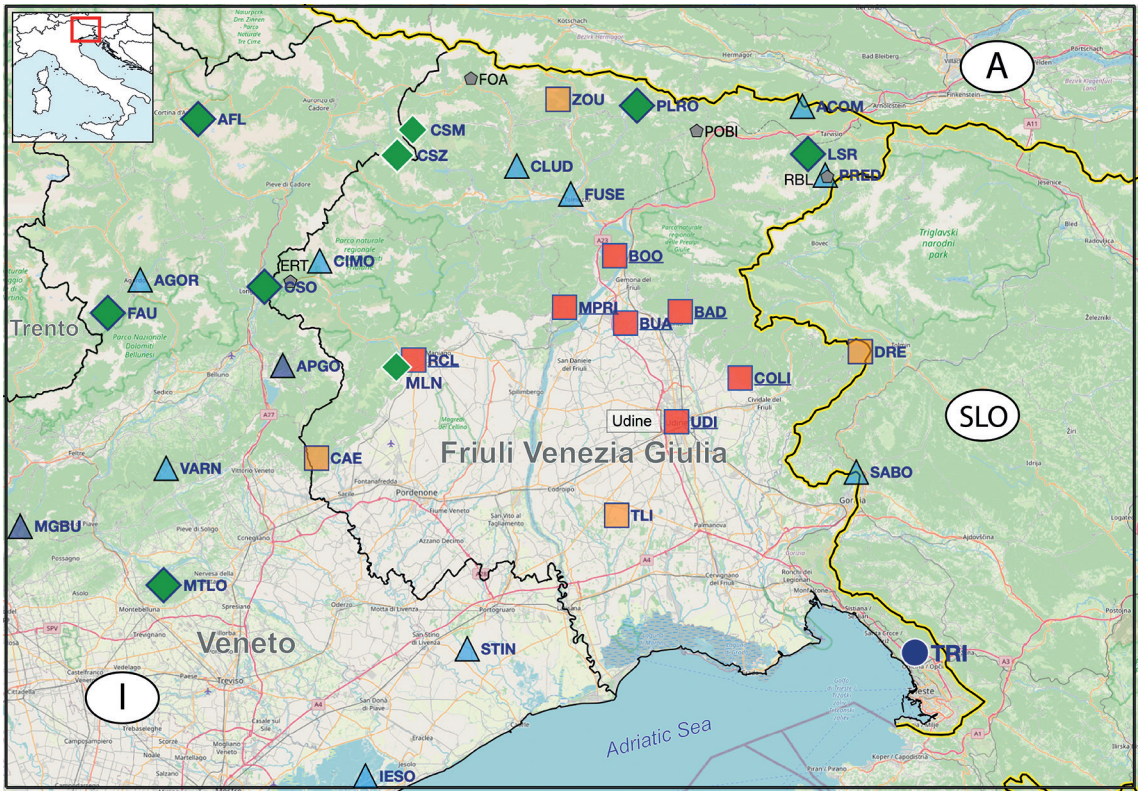

Fig. 6 - Historical evolution of the OX network: first core from 1977 (red squares); from 1983 (orange squares); from 1988 (green diamonds); from 2000 (blue triangles); stations with local recording (small pentagons). The WWSSN station of Trieste (TRI), active since 1963, is the blue circle.

service interruption, from 4 December 1990 to 21 May 1991 (Fir in Fig. 5), and the moving of the headquarter from the city centre of Udine to the current location in a neighbouring municipality. A new digital acquisition system (Lennartz Mars 88) was installed in 1994-1995 (2D in Fig. 5) but it was limited in the frequency band for data transmission: waveforms were recorded if the signal-to-noise ratio exceeded a threshold at any station, instead of exceeding it at least at three stations, as before. Since 2000, the data acquisition conditions have been enhanced and equipped with Lennartz LE-3DLite seismometers with an improvement in triggering and in the quality of the recorded data (Trg in Fig. 5). In 2006, the Antelope® BRTT automatic acquisition and location system was adopted as routine management and processing system (Ant in Fig. 5). From 1995, the short-period network was expanded with broadband stations. The velocimeters are mostly Nanometrics Trillium (120 s) and Streckeisen STS-2 (120 s) combined with Kinemetrics Quanterra Q330 dataloggers. The accelerometers are almost all Kinemetrics Episensor FBA ES-T. More details are available at the RTS web portal (https://rts.crs.inogs.it/it/project/1_mappa.html) and more information can be found in Priolo *et al*. (2005) and Bragato *et al*. (2021).

2.2.3. Changes in the real-time data processing

The Antelope® BRTT software package is a system of software modules developed for real-time seismic acquisition, automated detection, processing (e.g. picking, association, location, magnitude estimation), and data storage. An accurate choice of the Antelope® setting parameters is necessary to ensure the best performance of the real-time system, which means the most accurate location for the earthquakes (above the alarm threshold), avoiding any false event. This work of tuning was performed on 2011-2012 data, focused on the detection and association modules, and summarised in Moratto and Sandron (2015).

The data processing based on the new Antelope setting was also applied to the year 2010 (M&S in Fig. 5). The new setting of the Antelope system leads to a clear increase of the number of earthquakes located in the studied area (see Fig. 3) with a lowering of *Mc* with respect to the previous two decades but higher than in the first years (Fig. 5). This aspect has been investigated considering a smaller area of central Friuli, where the initial stations were located (Fig. 7a): *Mc* has been computed also in this area (Fig. 7b) as well as in the remaining external sector (Fig. 7c). It can be seen that the *Mc* trend in central Friuli (black line in Fig. 7b) is similar to that in the whole study region (Fig. 5) with a very slightly lower *Mc* value in the first years than after 2011. This slightly larger *Mc* value in the last decade than that in the 1977-1982 period can be justified by the easier identification of the signal in the noise with the correct settings of the digital Antelope system. It is suggested, then, that some earthquake signals were confused in the natural and/or instrumental noise recorded analogically, and a shorter than real coda duration was detected. This aspect is well-evidenced in the background of the *Mc* curve, where the number of events in each magnitude class is reported (Fig. 7b), and the large number of very small quakes is shown.

The analysis of the temporal trend of the *Mc* value in the area external to central Friuli (black curve in Fig. 7c) shows a light increase till 2001 and a sharp decrease after 2010, in agreement, but more evident, with respect to the *Mc* curve of the inner sector (black curve in Fig. 7b) and evidenced in the number of events in each magnitude class (red spots on the background of the *Mc* curve). The evident detection deterioration in the 1988-1993 period visible in both curves of Fig. 7, as well as in the cumulative curve of Fig. 5, can be justified by the insufficient performance of the first digital acquisition system, with a trigger set to only three stations (1D in Fig. 5), replaced later by a system with a trigger set to all stations (2D in Fig. 5).

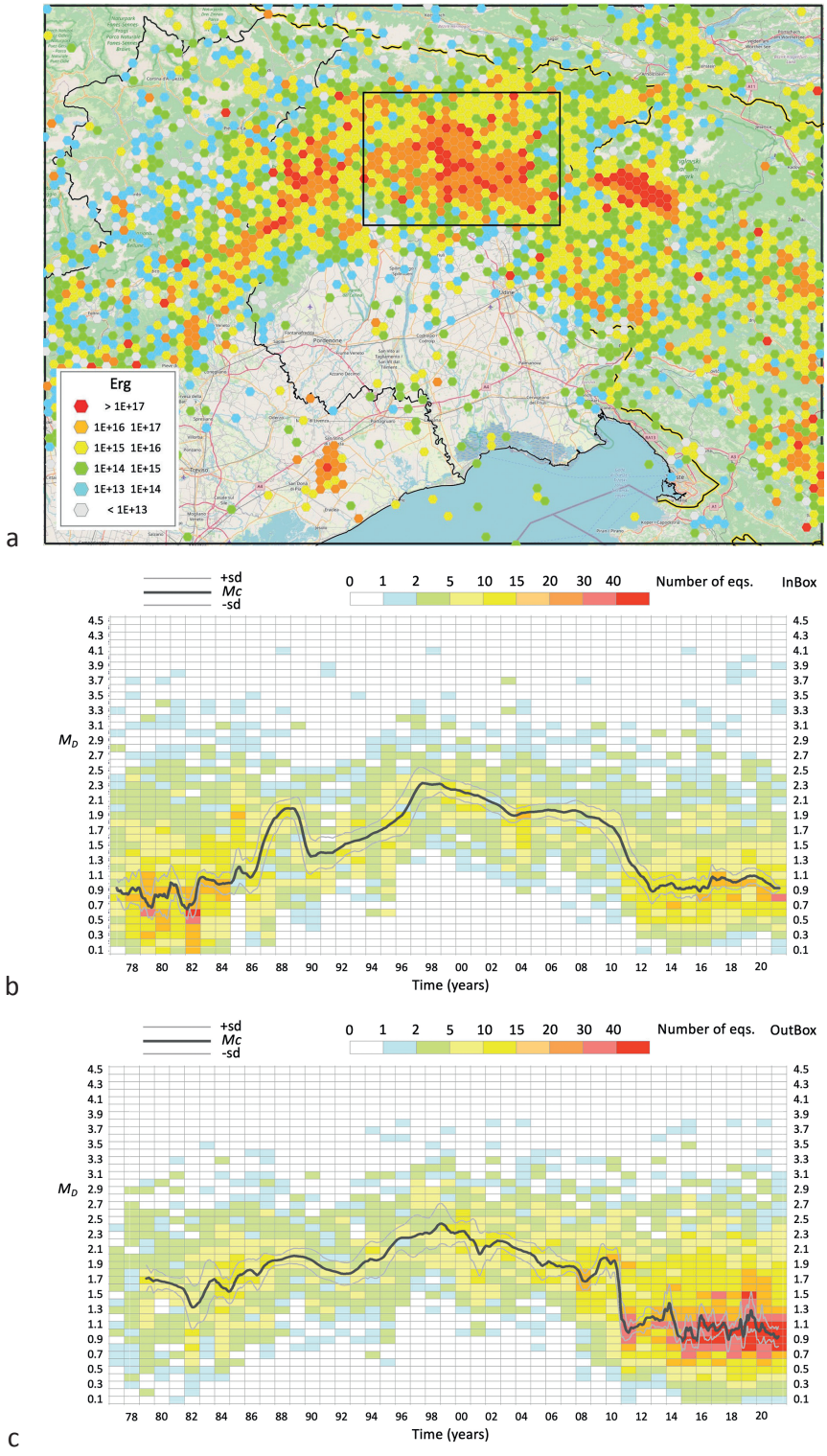

Fig. 7 - Cumulative seismic energy released in the period 6 May 1977 - 31 December 2021 from the OX network catalogue (a). The box indicates central Friuli, the remaining area represents the external region. *Mc* synoptic overview over time (1977-2021): *Mc* (obtained by the maximum curvature technique) is the dark grey line drawn over a counterplot of earthquakes per year binned in 0.1 magnitude classes, in central Friuli (b) and in the external region (c).

2.3. The regional b-value

One important parameter in earthquake statistics is the *b*-value of the G-R law, that is, basically, the slope of the FMD.

Recall *b* is typically equal to 1.0 in seismically active regions. This means that, for every *M*-magnitude event, there will be 10 (*M*-1)-magnitude quakes and 100 (*M*-2)-magnitude quakes. Variation with a *b*-value in the range 0.5 to 1.5 depends on the tectonic environment of the region. A notable exception can be observed during earthquake sequences, when the *b*-value can become as high as 2.5, indicating an even greater proportion of small quakes to large ones.

Fig. 8a shows the *b*-value trend for the entire data set (declustered OX network catalogue) calculated using the MAXC technique (Wiemer, 2001) implemented in the software package Zmap [version 7.1: http://www.seismo.ethz.ch/en/research-and-teaching/products-software/software/ZMAP/, Reyes and Wiemer (2019)]. As in the case of *Mc*, the first years after the installation of the network show a rather constant behaviour as well as the last decade, after 2010. The two periods, 1977-1983 and 2011-2021, respectively, have *b*-values that differ little (Fig. 8b), as in the case of *Mc*. In the early 1980s, the *b*-value was 0.65 (+/-0.12), from 2010 onwards it seems to be stabilised, with small fluctuations, around 0.84 (+/-0.08), in both cases rather low but in agreement with the average value during the whole period 1977-2021, i.e. 0.71 (+/-0.05). It must be said that the maximum likelihood method, applied for the *b*-value computations, heavily penalises the high magnitude rates, highlighting a probable lack of low magnitude events in the OX network catalogue (an *Mc* around 2.0, instead of 0.6, seems more reasonable for the period 1977-1983, see Fig. 8b).

The *a*-value of the recent years (3.47) is higher than that of the initial period (2.87) but considering a higher *Mc*, as suggested, the two values would be very similar (see Fig. 8b).

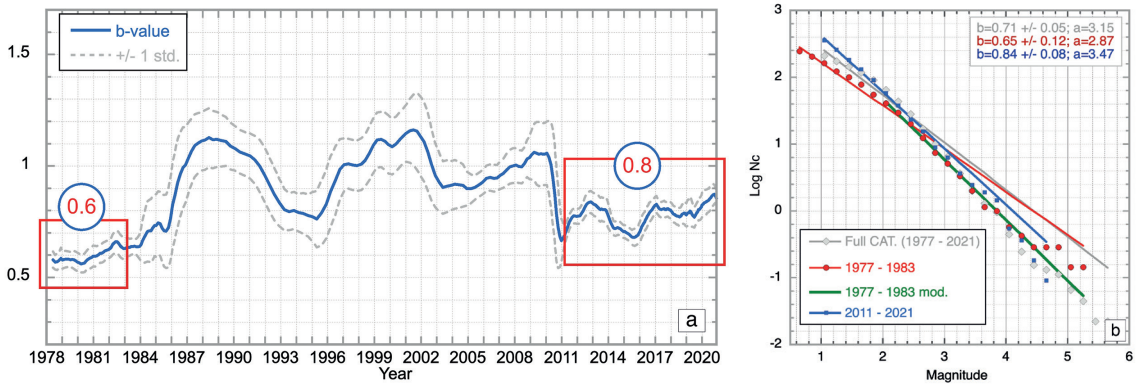

Fig. 8 - *b*-value: a) synoptic overview over time (1977–2021) (grey line; maximum curvature technique, Zmap); b) FMD for the two periods 1977-1983 (red) and 2011-2021 (blue); the green line represents the FDM 1977-1983 with *Mc*=2.0.

3. Seismicity in north-eastern Italy during the early 21st century (2000-2021)

The general picture of the seismicity recorded by the OX network since 1977 (Fig. 7a) is very similar to that of the 20th century (Fig. 2) as the main energy release occurred during the 1970s. A detailed description of the seismicity in the early years of the 21st century follows.

3.1. The first decade (2000-2009)

The seismicity of this area since the years 2000s, represented in terms of energy (see previous chapter), is fairly weak with only three isolated events that exceeded M_D 4.0. On the other hand, an improvement in the acquisition system and a considerable density of stations in the OX network allow the recording of many small-magnitude earthquakes. The zones where the greatest amount of seismic energy was released are outlined rather intuitively (Fig. 9): the thrust belt of the eastern Southern Alps and the Dinaric strike-slip system of western Slovenia. More precisely, Fig. 9 shows a bulk of earthquakes in central Friuli with a few clusters, one of which is related to the 2002 Mt. Sernio event (Table 3), a narrow SW-NE alignment of foci along the Veneto piedmont belt, and a more scattered epicentre distribution, tentatively suggesting an NW-SE Dinaric alignment, in Slovenia. There, the sequence following the 2004 Bovec event is clearly visible (Bressan *et al.*, 2009).

3.2. The second decade (2010-2021)

Earthquakes located by the OX network in the second decade of the 21st century appear much larger in number and more diffuse in the study region than in the previous years (Fig. 10). This is certainly due to the important improvements introduced in event detection. As mentioned, the real-time automatic detection, alerting and location system is implemented through the Antelope® BRTT software package gradually introduced since 2005. A careful choice

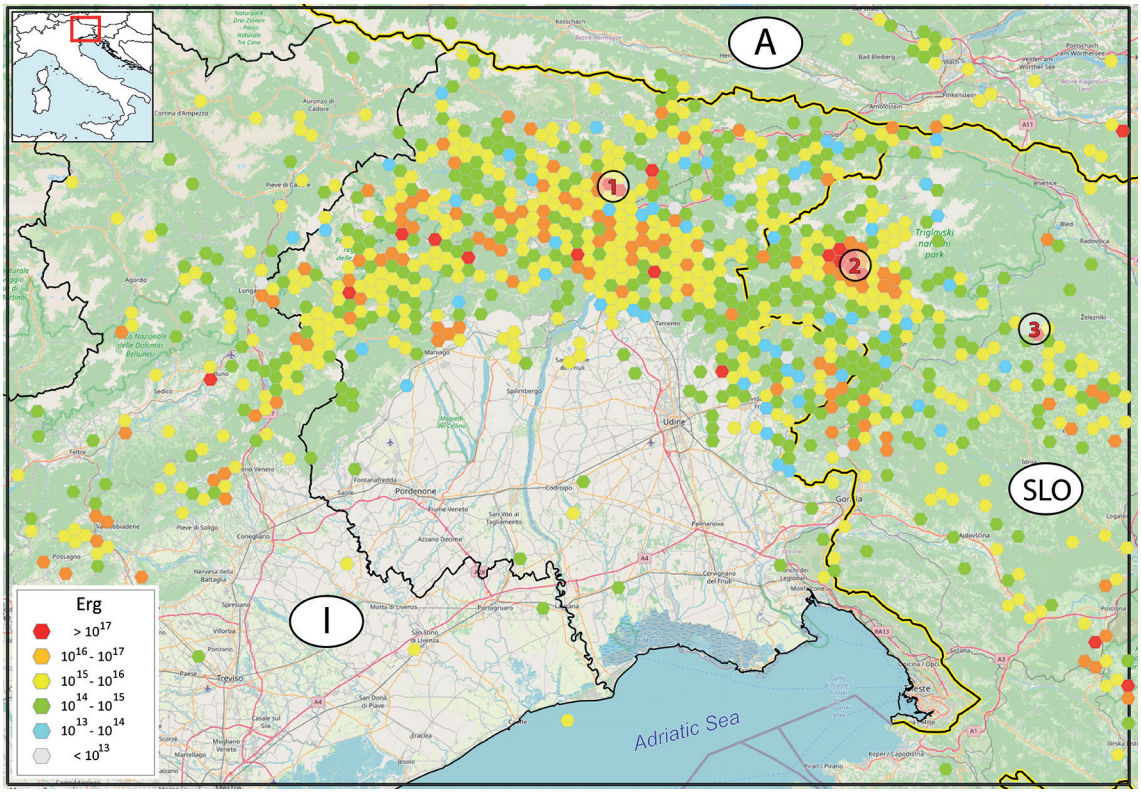

Fig. 9 - Cumulative seismic energy released in the period 1 January 2000 - 31 December 2009 from the OX network catalogue. Earthquakes with an M_D larger than, or equal to, 4.0, listed in Table 3, are highlighted in numbered circles.

of Antelope® setting parameters, necessary to guarantee the best performance of the system in real-time and avoid any false event, was pursued in 2010 (Moratto and Sandron, 2015). The fine-tuned parameters were validated on earthquakes that occurred in 2010, and since that date, the setup has been in place.

Table 3 - Earthquakes with an M_D larger than, or equal to, 4.0 occurring in north-eastern Italy and western Slovenia from 1 January 2000 to 31 December 2009. The data are extracted from the OX network catalogue.

No.	Date	Or. Time	Lat. N (°)	Lon. E (°)	M_D	Place
1	2002-02-14	03:18:02	46.426	13.100	4.9	Mt. Sernio, Friuli
2	2004-07-12	13:04:06	46.305	13.640	5.1	Bovec, Slovenia
3	2005-01-14	07:58:11	46.207	14.039	4.1	Podbrdo, Slovenia

In any case, the general features of the epicentre distribution repeat those of the previous years with the well-known alignment along the Southalpine piedmont belt and scattered seismicity in Slovenia where, only in the Bovec area, is a Dinaric alignment visible, generated by the two sequences of 2015 and 2020 (Table 4). The Southalpine active belt seems slightly larger than that pointed out in the previous years, especially in the Veneto region (Figs. 2 and 9) but, according to the cell geometry, the energy released in the last decade does not seem

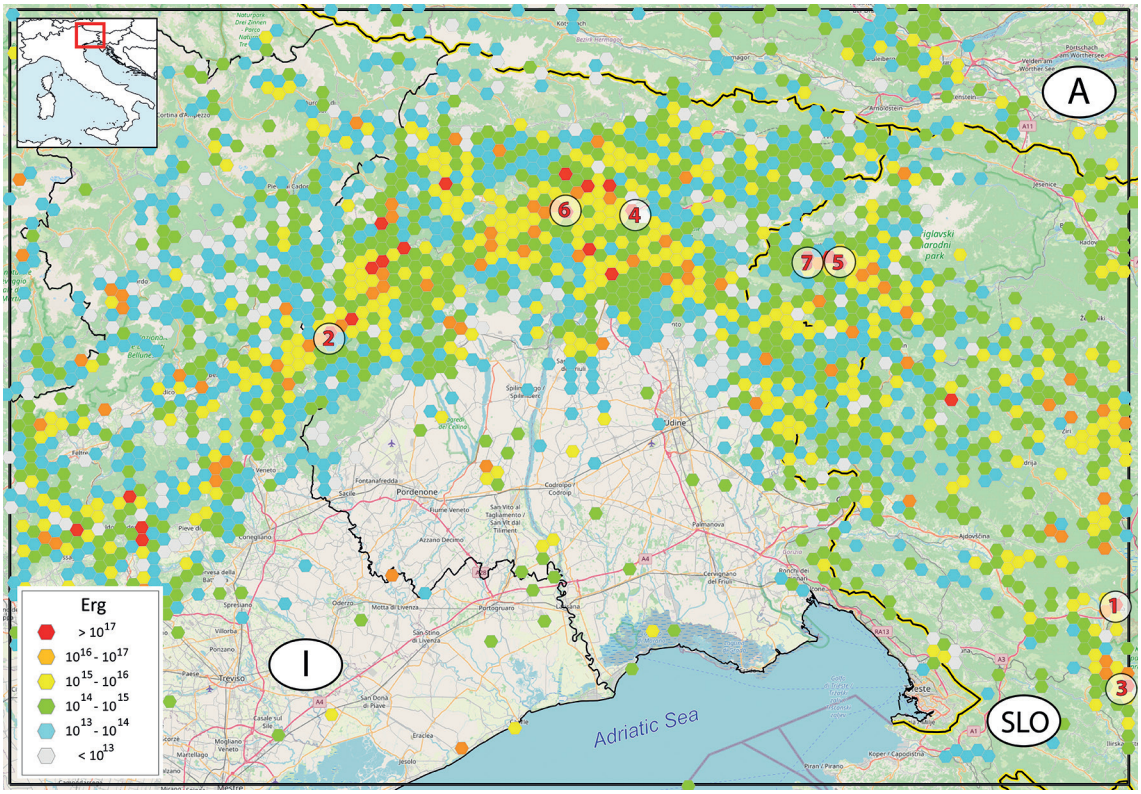

Fig. 10 - Cumulative seismic energy released in the period 1 January 2010 – 31 December 2021 from the OX network catalogue. Earthquakes with an M_D larger than, or equal to, 4.0, listed in Table 4, are highlighted in numbered circles.

more intense than that of the previous one (compare the yellow and red dots in Figs. 9 and 10). Furthermore, Fig. 10 shows low-energy cells that appear in low seismicity areas such as the Friuli plain and Slovenia.

Table 4 - Earthquakes with an M_D larger than, or equal to, 4.0 occurring in north-eastern Italy and western Slovenia from 1 January 2010 to 31 December 2021. The data are extracted from the OX network catalogue.

No.	Date	Or. Time	Lat. N (°)	Lon. E (°)	M_D	Place
1	2010-01-15	14:20:54	45.7810	14.2210	4.0	Postojna, Slovenia
2	2012-06-09	02:04:08	46.1960	12.4620	4.4	Barcis, Friuli
3	2014-04-22	08:58:27	45.6520	14.2400	4.7	Knezak, Slovenia
4	2015-01-30	00:45:49	46.3880	13.1490	4.1	Moggio Udinese, Friuli
5	2015-08-29	18:47:03	46.3140	13.6060	4.3	Bovec, Slovenia
6	2019-06-14	13:57:24	46.3955	12.9933	4.0	Verzegnis, Friuli
7	2020-07-17	02:50:57	46.3137	13.5337	4.2	Bovec, Slovenia

Several studies have been performed over the years using the tomographic inversion to investigate the crust structure of Friuli (Gentile *et al*., 2000), to characterise the stress and strain distribution (Bressan *et al*., 1998, 2003), and to analyse the fracture pattern (Bressan *et al*., 2016). The results show that the upper crust is largely heterogeneous, due to the superposition of different tectonic phases, and characterised by discontinuous blocks, marked by sharp lateral variations of the velocity of the seismic waves where the earthquakes mainly occur, but without a clear concentration on planar structures.

The results of a study by Bressan and Bragato (2009) indicate that the deformation pattern in north-eastern Italy and western Slovenia is heterogeneous with a significant strain partitioning among the deforming belts. More precisely, the belts located in the western part are undergoing a compressional strain that is changing orientation from NW-SE to NNW-SSE. The prevailing mode of deformation of the northern and eastern belts is related to a dextral strike-slip motion, along directions switching from NNE-SSW to NW-SE. The deformation geometry of the belts located in the central part of the study area is mainly compressional and N-S oriented.

Moreover, the characteristics of the seismicity have been studied with specific analyses of the seismic sequences, especially in the preparation of main events. Gentili and Bressan (2007) found that the spatial-temporal pattern of the seismicity preceding five moderate earthquakes ($M_D \geq 4.1$), in northern Friuli and in western Slovenia, suggests that the seismicity anomalies, like quiescence and foreshock activation, seem less evident than those preceding the severe earthquakes. Peresan and Gentili (2018) demonstrated that the earthquake clusters in north-eastern Italy had distinct preferential geographic locations and identified two areas that differ substantially in the examined clustering properties. Specifically, burst-like sequences are associated with the north-western sector and swarm-like sequences with the south-eastern part of the study area.

4. Calibration of the duration magnitude

Historically, the OX network catalogue reported the magnitude value expressed in terms of M_D. Currently, it still reports this value, but since 2015 it also includes the magnitude value expressed in terms of M_L, i.e. calculated from the amplitudes of the filtered waveforms for the

Wood Anderson seismometer, corrected for the station residuals and attenuation (Bragato and Tento, 2005).

After the pioneering studies of Suhadolc (1978) and Rebez and Renner (1991), an attempt to calibrate the M_D on the available values of the M_L calculated by the Wood Anderson seismometer of the WWSSN TRI station, still in operation (Sandron *et al*., 2015), was performed by Sandron *et al*. (2018). In that work, new individual station equations and an overall median (network) equation were derived with the intent, eventually, to use them for a re-evaluation of the entire catalogue in a homogeneous manner. Their obtained network relation was:

$$M_D\ (\cong M_L) = 2.96 \log t - 3.10 \quad R = 0.99 \tag{1}$$

where M_L is the TRI M_L, and t is the total duration in seconds [from the onset of the first P-arrival to the point where the trace amplitude becomes lost in the noise (see Real and Teng, 1973)]. The range of applicability of this relation is stated as $1.8 \leq M_D \leq 5.0$. Rebez and Renner (1991) also introduced in their work a coefficient for the station-to-event epicentral distance correction, but underlining, at the same time, that it is very small (in the order of 10^{-3}) and that its contribution can be neglected [see also Lee *et al*. (1972)]. Instrument sensitivity has been ignored as well because almost all the instruments are identical and the instrument amplification is adjusted according to the background noise level, thereby compensating for the effects of local site conditions (see Lee *et al.*, 1972).

However, the conclusion of the Sandron *et al*. (2018) study was, for their available data (grey diamonds in Fig. 11), that the calibration of M_D on M_L was robust only in the magnitude range $2.0 < M_D < 5.0$. Notwithstanding the limited number of low-magnitude events, the converted M_D values were, however, in good agreement with those calculated by the Slovenian ARSO agency (http://potresi.arso.gov.si) even for magnitudes as low as $M_D = 1.0$.

Taking advantage of the availability of a large new data set of M_L, routinely calculated today in parallel with the historical M_D (published on the RTS portal along with their respective readings), we have integrated the Sandron *et al*. (2018) data set with (M_L – durations) pairs in the magnitude range 0.0-3.5 (solid blue circles in Fig. 11). As in Sandron *et al*. (2018), events with an M_L larger than 5.0 have not been used because of the difficulties encountered in assessing the related durations. We have, then, calculated a new regression on the entire data set (green line in Fig. 11), which takes the form:

$$M_D\ (\cong M_L) = 2.272\ (+/-0.006) \log t - 1.839\ (+/-0.009). \tag{2}$$

In addition, we have also computed an orthogonal regression (red line in Fig. 10):

$$M_D\ (\cong M_L) = 2.416\ (+/-0.004) \log t - 2.039\ (+/-0.008) \tag{3}$$

considering that the uncertainties in both the estimation of the durations in seconds of the event and the estimation of the amplitudes of the waveforms, automatically processed within the same software package, are wholly comparable. In addition, should there be a revision of the seismologist on duty, they will intervene equally on both fronts and we can ultimately assume that both groups of estimates operate within a common uncertainty range. We propose the $0.0 \leq M_D \leq 5.0$ range of applicability for both relations.

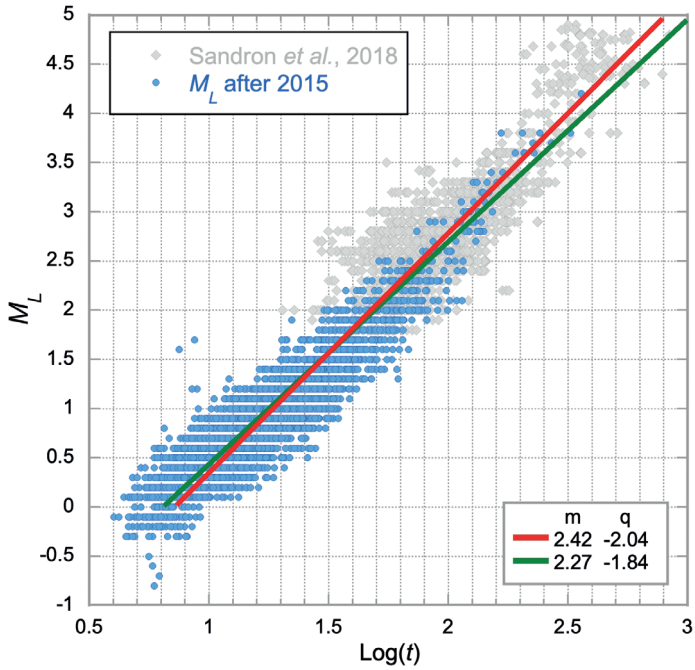

Fig. 11 - Calibration of M_L vs. ground motion duration [log(*t*)] on the merged data set of Sandron *et al*. (2018) (grey diamonds) and OX network catalogue after 2015 (solid blue dots). The slope (*m*) and intercept (*q*) are reported in the legend: orthogonal fit (red line); linear fit (green line).

Fig. 12 shows the comparison between the original M_L and the M_D values, respectively, as available in the OX network catalogue (at the RTS website, Fig. 12a), calculated by Eq. 1 (Fig. 12b), and calculated by Eq. 3 (Fig. 12c), limited to the period 2015-2021 for which, as mentioned above, both M_L and M_D are available in the OX network catalogue. Considering M_L (*x*-axis) as the reference, we can see that the OX M_D values (Fig. 12a) for the same event are circa 0.3 greater than the M_L ones in the definition range of the relationship as well as for lower values. The M_D values obtained by applying the Sandron *et al*. (2018) regression (Eq. 1) agree with the M_L values inside the definition range well, but underestimate the low magnitude events (Fig. 12b). The M_D values obtained by applying the new regression (Eq. 3) agree with the higher magnitude values well (see regression lines and data points in Fig. 11 for the whole data range), which were already present in the data set used by Sandron *et al*. (2018), and, at the same time, showing a lower slope, also agree well with the lower magnitude values ($M_D < 2.0$), to a large degree related to recent earthquakes (Fig. 12c) not present in the data set used by Sandron *et al*. (2018).

5. Conclusions

Every technological transition always leads to an improvement but this is not always immediate. In the specific case of the operation and ability of the OX network to adequately locate seismicity, the transition from the analog acquisition of the 1970s and 1980s to the digital one of the 1990s did not bring immediate benefits. This surprising evidence could be motivated by the difficulties encountered in defining the suitable setting for the trigger parameters during the first years. This study demonstrates that in the first (analog) period of the network operation,

the ability to detect and locate earthquakes was excellent. Subsequently, with the advent of the transition to digital data acquisition, the network performance has decreased. It should be remembered that the first digital systems had reduced acquisition dynamics, that the available data transmission frequencies were only a few, and, consequently, the trigger system, which governs the mechanisms of recording and subsequent location of the event, was necessarily reduced. The result is a long period when the network did not locate all the low-magnitude earthquakes. Only in the last decade (from 2010-2011) has the system reached and exceeded the performance of the first (analog) period.

The continuous acquisition, the improved conditions of data transmission using the coverage of the mobile phone network (GPRS, 2G, and 3G), and the refinement of the parameters regulating the automatic earthquake detection system of the Antelope BRTT software have led to a clear improvement in the overall capacity of the network.

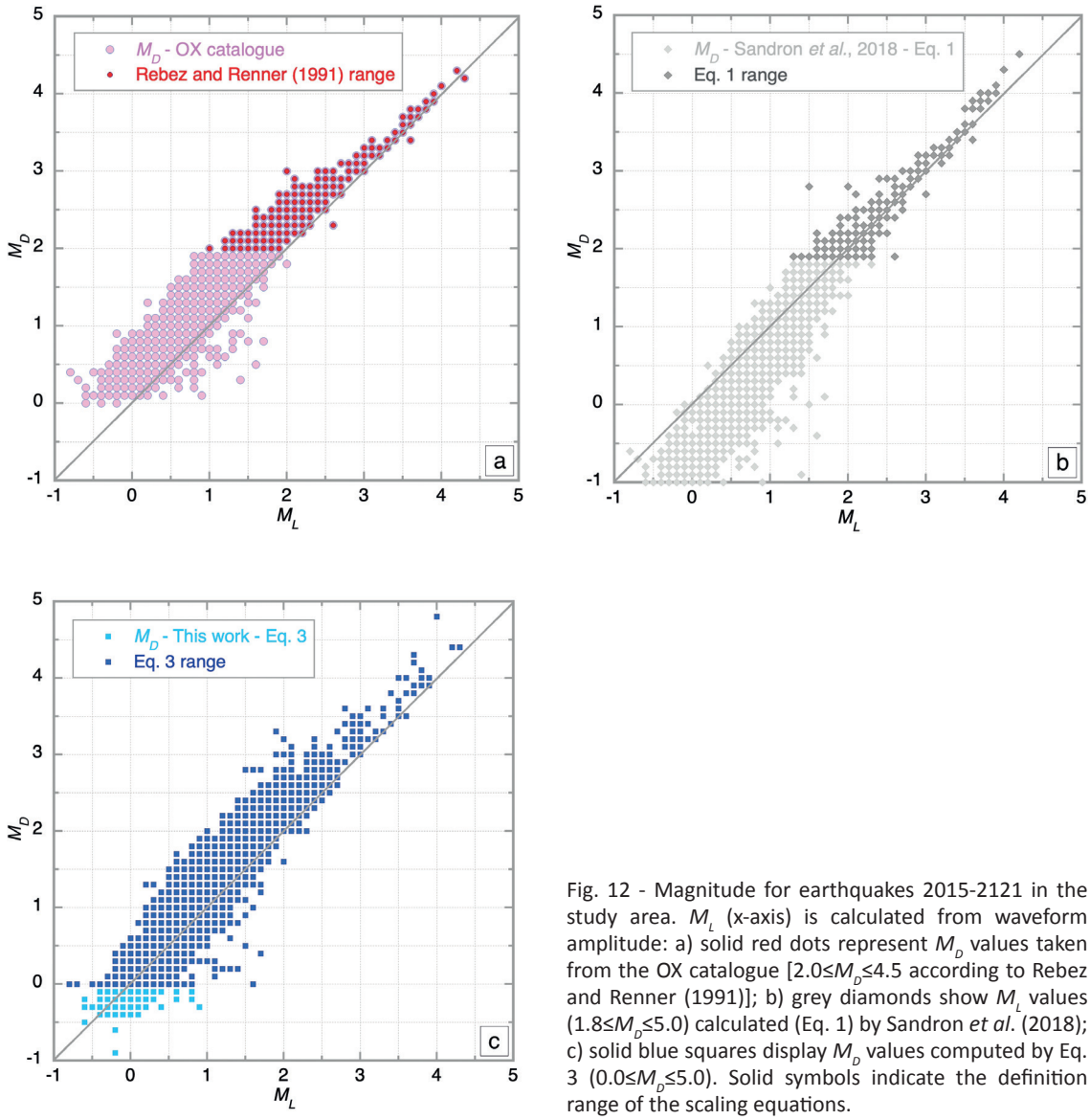

Fig. 12 - Magnitude for earthquakes 2015-2121 in the study area. M_L (x-axis) is calculated from waveform amplitude: a) solid red dots represent M_D values taken from the OX catalogue [$2.0 \leq M_D \leq 4.5$ according to Rebez and Renner (1991)]; b) grey diamonds show M_L values ($1.8 \leq M_D \leq 5.0$) calculated (Eq. 1) by Sandron *et al*. (2018); c) solid blue squares display M_D values computed by Eq. 3 ($0.0 \leq M_D \leq 5.0$). Solid symbols indicate the definition range of the scaling equations.

Naturally, technology is progressing and with the spread of greater coverage of cellular networks, access to sustainable costs of satellite technology, the improvement of computing capacity, and the sensitivity and reliability of sensors, we are heading towards an improved capacity to study the earthquake phenomenon.

Since 2010, the monitoring network operated by OGS has reached a consolidated level in terms of geometry and number of stations. At the same time, the entire data acquisition and processing system are homogeneous and wholly robust. This is demonstrated by the analysis performed on the quality of the hypocentre locations (Fig. 4) and the variations in the capability of the network in event detection (Fig. 5).

The analysis of the seismicity during the last two decades has confirmed a general similarity with that observed during the previous years, with the active Southalpine belt showing its largest seismicity in central Friuli and diffuse earthquakes related to the Dinaric front (Figs. 2, 7, 9, and 10). It is quite interesting that the chosen new representation of the seismicity, in terms of energy released on a regular grid, does not highlight epicentre alignments. If this is reasonable in the Southalpine chain, characterised by thrust faults, this is unexpected in Slovenia, where transcurrent faults dominate. Of interest is also the investigation of the *b*-value variations in time (Fig. 8) because of the large fluctuations identified.

Moreover, the availability of a statistically significant data set has allowed us to define a robust calibration between M_D and M_L, such that we are able to provide a homogeneous complete catalogue in terms of M_L from the network beginnings (1977) to the present day.

All of the low-magnitude seismicity, which could be defined as background seismicity, that arose since 2010 would likely have been detected also in the previous years adopting the network's current detection standards. It is, therefore, not a natural phenomenon, i.e. a systematic increase in seismicity as we would be led to believe, because above the M_D 2.5 threshold (the OX network alert threshold for Civil Protection purposes), the number of earthquakes is almost constant throughout the entire catalogue.

Acknowledgments. All maps are obtained by the Cartographica software and the background is taken from Open Street Map. The OX seismometric network is managed by OGS with financial contribution from the Regione Autonoma Friuli Venezia Giulia. Many thanks to Odysseas Galanis and Dimcho Solakov, who improved the original manuscript with helpful comments.

REFERENCES

Andreotti G.; 1937: *Il terremoto del 18 Ottobre 1936*. Mem. Reale Ist. Veneto Sci. Lett. Arti, 30, 3-24.

Bajc J., Aoudia A., Sarao A. and Suhadolc P.; 2001: *The 1998 Bovec-Krn mountain (Slovenia) earthquake*. Geophys. Res. Lett., 28, 1839-1842.

Bragato P.L. and Tento A.; 2005: *Local magnitude in northeastern Italy*. Bull. Seismol. Soc. Am., 95, 579-591.

Bragato P.L., Comelli P., Saraò A., Zuliani D., Moratto L., Poggi V., Rossi G., Scaini C., Sugan M., Barnaba C., Bernardi P., Bertoni M., Bressan G., Compagno A., Del Negro E., Di Bartolomeo P., Fabris P., Garbin M., Grossi M., Magrin A., Magrin E., Pesaresi D., Petrovic B., Plasencia Linares M.P., Romanelli M., Snidarcig A., Tunini L., Urban S., Venturini E. and Parolai S.; 2021: *The OGS - northeastern Italy seismic and deformation network: current status and outlook*. Seismol. Res. Lett., 92, 1704-1716, doi: 10.1785/0220200372.

Bressan G. and Bragato P.L.; 2009: *Seismic deformation pattern in the Friuli-Venezia Giulia region (north-eastern Italy) and western Slovenia*. Boll. Geof. Teor. Appl., 50, 255-275.

Bressan G., Snidarcig A. and Venturini C.; 1998: *Present state of tectonic stress of the Friuli area (eastern Southern Alps)*. Tectonophys., 292, 211-227.

Bressan G., Bragato P.L. and Venturini C.; 2003: *Stress and strain tensors based on focal mechanisms in the seismotectonic framework of the eastern Southern Alps*. Bull. Seismol. Soc. Am., 93, 1280-1297.

Bressan G., Gentile G.F., Perniola B. and Urban S.; 2009: *The 1998 and 2004 Bovec-Krn (Slovenia) seismic sequences: aftershock pattern, focal mechanisms and static stress changes*. Geophys. J. Int., 179, 231-253, doi: 10.1111/j.1365-246X.2009.04247.x.

Bressan G., Ponton M., Rossi G. and Urban S.; 2016: *Spatial organization of seismicity and fracture pattern in NE Italy and W Slovenia*. J. Seismol., 20, 511-534, doi: 10.1007/s10950-015-9541-9.

Bressan G., Barnaba C., Bragato P.L., Peresan A., Rossi G. and Urban S.; 2019: *Distretti sismici del Friuli Venezia Giulia*. Boll. Geof. Teor. Appl., 60, s1-s74, doi: 10.4430/bgta0300.

Camassi R., Caracciolo C.H., Castelli V. and Slejko D.; 2011: *The 1511 Eastern Alps earthquakes: a critical update and comparison of existing macroseismic datasets*. J. Seismol., 15, 191-213, doi: 10.1007/s10950-010-9220-9.

Caracciolo C.H., Slejko D., Camassi R. and Castelli V.; 2021: *The eastern Alps earthquake of 25 January 1348: new insights from old sources*. Bull. Geoph. Ocean., 62, 335-364, doi: 10.4430/bgo00364.

Carulli G.B. and Slejko D.; 2005: *The 1976 Friuli (NE Italy) earthquake*. Giornale di Geologia Applicata, 1, 147-156.

Carulli G.B., Nicolich R., Rebez A. and Slejko D.; 1990: *Seismotectonics of the Northwest External Dinarides*. Tectonophys., 179, 11-25.

Cavasino A.; 1929: *Il terremoto nelle Prealpi Carniche orientali del 27 marzo 1928*. Boll. Soc. Sismol. Ital., 28, 77-100.

Cergol M. and Slejko D.; 1991: *I terremoti del 1511 e del 1690 nelle Alpi Orientali.* In: Albini P. and Barbano M.S. (eds), Atti del Convegno GNDT 1990 Macrosismica, Pisa, Italy, vol.2, pp. 69-91.

Del Ben A,. Finetti I., Rebez A. and Slejko D.; 1991: *Seismicity and seismotectonics at the Alps - Dinarides contact*. Boll. Geof. Teor. Appl., 33, 155-176.

Finetti I., Russi M. and Slejko D.; 1979: *The Friuli earthquake (1976-1977)*. Tectonophys., 53, 261-272.

Galadini F., Poli M.E. and Zanferrari A.; 2005: *Seismogenic sources potentially responsible for earthquakes with M ≥ 6 in the eastern Southern Alps (Thiene - Udine sector, NE Italy).* Geophys. J. Int., 161, 739-762.

Gentile G.F., Bressan G., Burlini L. and De Franco R.; 2000: *Three-dimensional VP and VP/VS models of the upper crust in the Friuli area (northeastern Italy).* Geophys. J. Int., 141, 457-478.

Gentili S. and Bressan G.; 2007: *Seismicity patterns before MD ≥ 4.1 earthquakes in the Friuli-Venezia Giulia (N.E. Italy) and western Slovenia areas*. Boll. Geof. Teor. Appl., 48, 33-51.

Gentili S., Sugan M., Peruzza L. and Schorlemmer D.; 2011: *Probabilistic completeness assessment of the past 30 years of seismic monitoring in northeastern Italy*. Phys. Earth Planet. Inter., 186, 81-96, doi: 10.1016/j.pepi.2011.03.005.

Giacchetti G., Iliceto V. and Slejko D.; 1987: *Approccio macrosismico al calcolo della risposta sismica locale nel Bellunese*. Geologia Tecnica, 2, 4-18.

Gortani M.; 1928: *Il terremoto del 27 marzo 1928 nelle Prealpi dell'Arzino (Friuli). Note geologiche*. L'Universo, 9, 1155-1210.

Guidoboni E., Ferrari G., Mariotti D., Comastri A., Tarabusi G., Sgattoni G. and Valensise G.; 2018: *CFTI5Med, Catalogo dei Forti Terremoti in Italia (461 a.C.-1997) e nell'area Mediterranea (760 a.C.-1500).* Istituto Nazionale di Geofisica e Vulcanologia (INGV), Roma, Italy, doi: 10.6092/ingv.it-cfti5.

Guidoboni E., Ferrari G., Tarabusi G., Sgattoni G., Comastri A., Mariotti D., Ciuccarelli C., Bianchi M.G. and Valensise G.; 2019: *CFTI5Med, the new release of the catalogue of strong earthquakes in Italy and in the Mediterranean area*. Sci. Data, 6, 80, doi: 10.1038/s41597-019-0091-9.

Husen S. and Hardebeck J.L.; 2010: *Earthquake location accuracy*. Community online Resource for Statistical Seismicity Analysis, 35 pp., doi: 10.5078/corssa-55815573.

Iurcev M., Pettenati F. and Diviacco P.; 2021: *Improved automated methods for near real-time mapping - application in the environmental domain*. Boll. Geof. Teor. Appl., 62, 427-454, doi: 10.4430/bgta0360.

Lee W.H.K. and Lahr J.C.; 1975: *HYPO71 (revised): a computer program for determining hypocenter, magnitude and first motion pattern of local earthquakes*. U.S. Geological Survey, Menlo Park, CA, USA, Open file report, 75-311, 113 pp., doi: 10.3133/ofr75311.

Lee W.H.K., Bennet R.E. and Meaghu K.L.; 1972: *A method of estimating magnitude of local earthquakes from signal duration.* U.S. Geological Survey, Menlo Park, CA, USA, Open file report, 72-223, 28 pp., doi: 10.3133/ofr72223.

Mignan A. and Woessner J.; 2012: *Estimating the magnitude of completeness for earthquake catalogs*. Community online Resource for Statistical Seismicity Analysis, 45 pp., doi: 10.5078/corssa-00180805.

Moratto L. and Sandron D.; 2015: *Optimazing the automatic location of the real-time Antelope® system in northeastern Italy*. Boll. Geof. Teor. Appl., 56, 407-424, doi: 10.4430/bgta0154.

Peresan A. and Gentili S.; 2018: *Seismic clusters analysis in northeastern Italy by the nearest-neighbor approach*. Phys. Earth Planet. Inter., 274, 87-104, doi: 10.1016/j.pepi.2017.11.007.

Peruzza L., Iliceto V. and Slejko D.; 1989: *Some seismotectonic aspects of the Alpago - Cansiglio area (N.E. Italy)*. Boll. Geof. Teor. Appl., 31, 63-75.

Peruzza L., Garbin M., Snidarcig A., Sugan M., Urban S., Renner G. and Romano M.A.; 2015: *Quarry blasts, underwater explosions, and other dubious seismic events in NE Italy from 1977 to 2013*. Boll. Geof. Teor. Appl., 56, 437-459, doi: 10.4430/bgta0159.

Poli M.E. and Zanferrari A.; 2018: *The seismogenic sources of the 1976 Friuli earthquakes: a new seismotectonic model for the Friuli area*. Boll. Geof. Teor. Appl., 59, 463-480, doi: 10.4430/bgta0209.

Poli M.E., Peruzza L., Rebez A., Renner G., Slejko D. and Zanferrari A.; 2002: *New seismotectonic evidence from the analysis of the 1976-1977 and 1977-1999 seismicity in Friuli (NE Italy)*. Boll. Geof. Teor. Appl., 43, 53-78.

Priolo E., Barnaba C., Bernardi P., Bernardis G., Bragato P.L., Bressan G., Candido M., Cazzador E., Di Bartolomeo P., Durì G., Gentili S., Govoni A., Klinc P., Kravanja S., Laurenzano G., Lovisa L., Marotta P., Michelini A., Ponton F., Restivo A., Romanelli M., Snidarcig A., Urban S., Vuan A. and Zuliani D.; 2005: *Seismic monitoring in northeastern Italy: a ten-year experience*. Seismol. Res. Lett., 76, 446-454.

Real C.R. and Teng T.; 1973: *Local Richter magnitude and total signal duration in southern California*. Bull. Seismol. Soc. Am., 63, 1809-1827.

Rebez A. and Renner G.; 1991: *Duration magnitude for the northeastern Italy seismometric network.* Boll. Geof. Teor. Appl., 33, 177-186.

Rebez A., Cecić I., Renner G., Sandron D. and Slejko D.; 2018: *Misunderstood "forecasts": two case histories from former Yugoslavia and Italy*. Boll. Geof. Teor. Appl., 59, 481-504, doi: 10.4430/bgta0244.

Reiter L.; 1990: *Earthquake hazard analysis: issues and insights*. Columbia University Press, New York, NY, USA, 254 pp.

Renner G.; 1995: *The revision of the northeastern Italy seismometric network catalogue*. Boll. Geof. Teor. Appl., 37, 329 pp.

Reyes C. and Wiemer S.; 2019: *ZMAP7: a refreshed software package to analyze seismicity*. In: Proc. 21st EGU General Assembly, Vienna, Austria, id. 13153, 1 p.

Rovida A., Locati M., Camassi R., Lolli B. and Gasperini P.; 2020: *The Italian earthquake catalogue CPTI15*. Bull. Earthquake Eng., 18, 2953-2984, doi: 10.1007/s10518-020-00818-y.

Rovida A., Locati M., Camassi R., Lolli B., Gasperini P. and Antonucci A.; 2022: *Catalogo Parametrico dei Terremoti Italiani (CPTI15), versione 4.0*. Istituto Nazionale di Geofisica e Vulcanologia (INGV), Roma, Italy, doi: 10.13127/CPTI/CPTI15.4.

Sandron D., Renner G., Rebez A. and Slejko D.; 2014: *Early instrumental seismicity recorded in the eastern Alps*. Boll. Geof. Teor. Appl., 55, 755-788, doi: 10.4430/bgta0118.

Sandron D., Gentile G.F., Gentili S., Saraò A., Rebez A., Santulin M. and Slejko D.; 2015: *The Wood-Anderson of Trieste (northeast Italy): one of the last operating torsion seismometers*. Seismol. Res. Lett., 86, 1645-1654, doi: 10.1785/0220150047.

Sandron D., Rebez A. and Slejko D.; 2018: *Calibration of the duration magnitude for the North-Eastern Italy Seismic Network (OX) on the basis of the revised local magnitudes of the Trieste station*. Boll. Geof. Teor. Appl., 59, 249-266, doi: 10.4430/bgta0237.

Slejko D.; 2018: *What science remains of the 1976 Friuli earthquake?* Boll. Geof. Teor. Appl., 59, 327-350, doi: 10.4430/ bgta0224.

Slejko D. and Rebez A.; 2002: *Probabilistic seismic hazard assessment and deterministic ground shaking scenarios for Vittorio Veneto (NE Italy)*. Boll. Geof. Teor. Appl., 43, 263-280.

Slejko D., Carulli G.B., Nicolich R., Rebez A., Zanferrari A., Cavallin A., Doglioni C., Carraro F., Castaldini D., Iliceto V., Semenza E. and Zanolla C.; 1989: *Seismotectonics of the eastern Southern Alps: a review*. Boll. Geof. Teor. Appl., 31, 109-136.

Slejko D., Camassi R., Cecic I., Herak D., Herak M., Kociu S., Kouskouna V., Lapajne J., Makropoulos K., Meletti C., Muco B., Papaioannou C., Peruzza L., Rebez A., Scandone P., Sulstarova E., Voulgaris N., Zivcic M. and Zupancic P.; 1999: *Seismic hazard assessment for Adria*. Ann. Geof., 42, 1085-1107.

Slejko D., Carulli G.B., Riuscetti M., Cucchi F., Grimaz S., Rebez A., Accaino F., Affatato A., Biolchi S., Nieto D., Puntel E., Sanò T., Santulin M., Tinivella U. and Zini L.; 2011: *Soil characterization and seismic hazard maps for the Friuli Venezia Giulia region (NE Italy)*. Boll. Geof. Teor. Appl., 52, 59-104.

Sugan M. and Peruzza L.; 2011: *Distretti sismici del Veneto*. Boll. Geof. Teor. Appl., 52, s3-s90, doi: 10.4430/ bgta0057.

Suhadolc P.; 1978: *Total durations and local magnitudes for small shocks in Friuli*. Boll. Geof. Teor. Appl., 20, 303-312.

Wiemer S.; 2001: *A software package to analyze seismicity: ZMAP*. Seismol. Res. Lett., 72, 373-382.

Corresponding author: Alessandro Rebez
Istituto Nazionale di Ocenografia e di Geofisica Sperimentale - OGS
Borgo Grotta Gigante 42c, 34010 Sgonico (TS), Italy
Phone: +39 040 2140250; e-mail: arebez@ogs.it